

# Transport in two-dimensional materials

Vassilios Vargiamidis

WCPM, University of Warwick, UK

# Outline

## Overview of graphene

- Crystal structure, band structure, Dirac cones, etc.
- Density of states

## Transport in silicene

- Tuning the charge conductance and transport gap
- Spin-resolved, valley-resolved, and charge conductances
- Near perfect spin and valley polarizations
- Topological phase transitions

## Possible applications

## Summary

# Overview of graphene

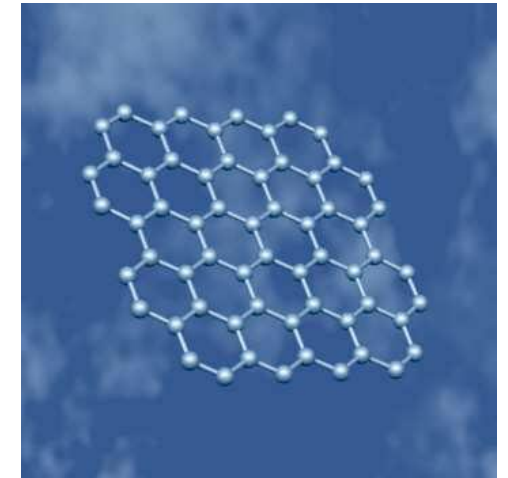
# Graphene pioneers (Nobel prize 2010)



Andrey Geim



Kostya Novoselov



Philip Kim

New 2D electron system (Manchester 2004)

Nanoscale electron system with *tunable properties*;  
Field-effect enabled by gating: tunable carrier density

1. very high mobilities in its suspended form:  $\mu \sim 200.000\text{cm}^2/(\text{V.s})$
2. ballistic transport over sub-micron distances:  $l \sim 1\mu\text{m}$
3. high thermal conductivity:  $\kappa=5000\text{W}/(\text{m.K})$ ,
4. chemically stable, very stiff, . . .

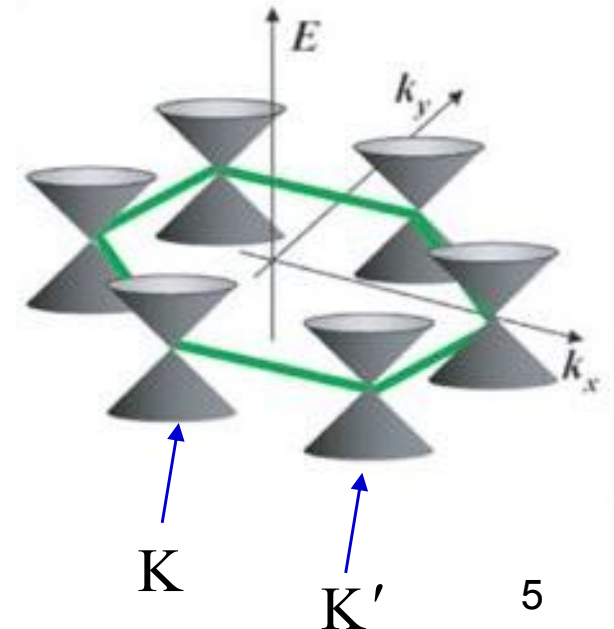
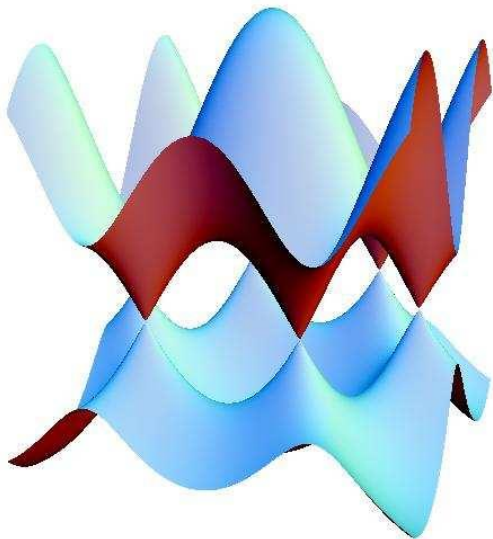
## Semimetal (zero bandgap): electrons and holes coexist

- Electronic energy dispersion: Dirac points
- Hexagonal BZ: 2 inequivalent points  $K$  and  $K'$  where carriers mimic relativistic massless Dirac particles
- **Linear energy dispersion** at  $K$  and  $K'$ : massless Dirac fermion model in 2D

$$E = \sqrt{m^2c^4 + p^2c^2}, \quad m \rightarrow 0$$

$$v_F = 10^6 \text{ m/s} = \frac{c}{300}$$

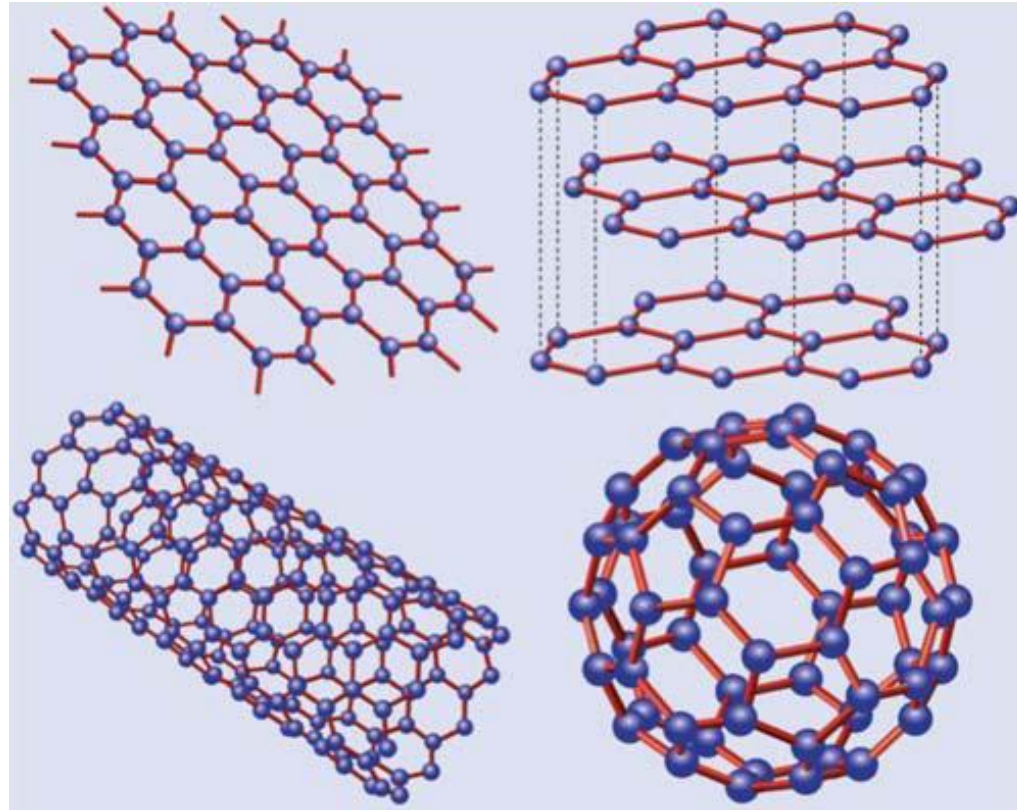
**Slow, but ultrarelativistic  
Dirac Fermions!**



# Graphene allotropes

2D Graphene:  
presumed not to  
exist in the free  
state

(2004) →



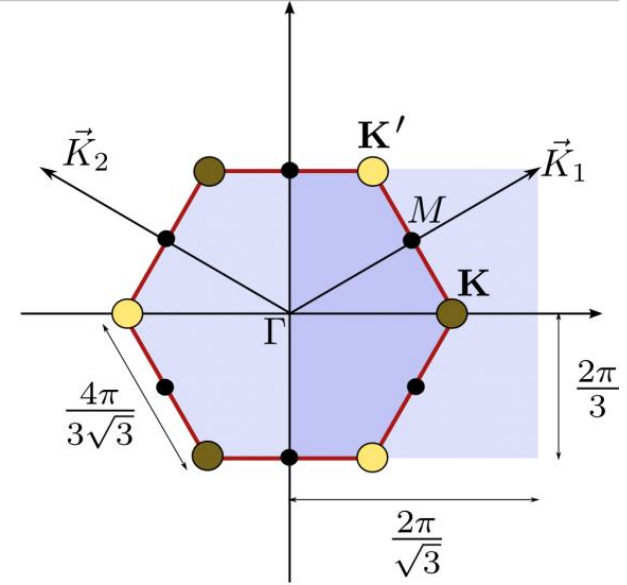
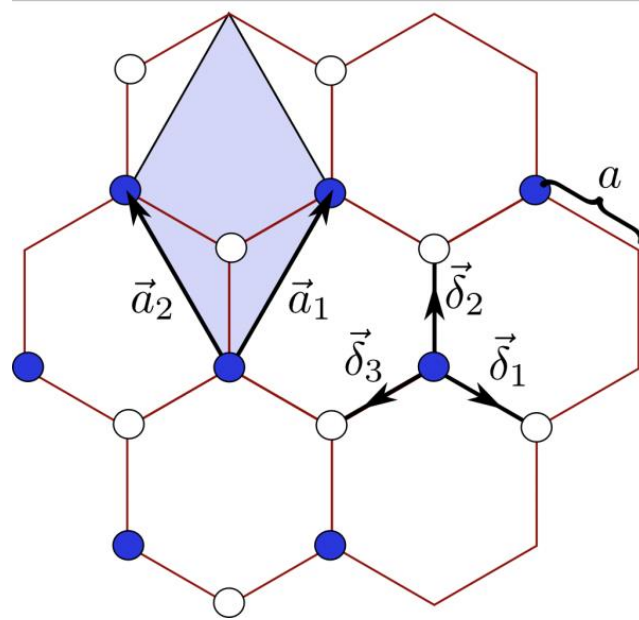
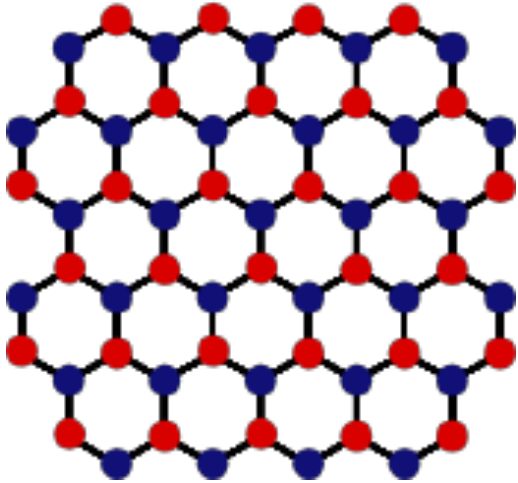
← 3D Graphite

↖  
1D Carbon Nanotube (1991)  
(rolled-up cylinder of graphene)

↖  
0D Fullerenes (“buckyball”)  
(1985)

# Graphene's honeycomb lattice

1<sup>st</sup> Brillouin zone



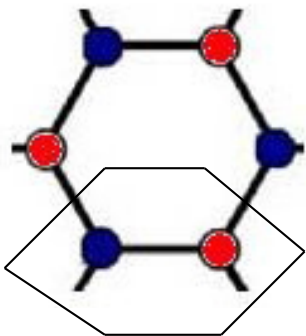
$$\vec{a}_1 = \frac{\alpha}{2}(\sqrt{3}, 3)$$

$$\vec{a}_2 = \frac{\alpha}{2}(-\sqrt{3}, 3)$$

$$\vec{K}_1 = \frac{2\pi}{3\alpha}(\sqrt{3}, 1)$$

$$\vec{K}_2 = \frac{2\pi}{3\alpha}(-\sqrt{3}, 1)$$

$$\alpha = 0.142 \text{ nm}$$



Unit cell

Inequivalent points  $\vec{K}$  and  $\vec{K}'$

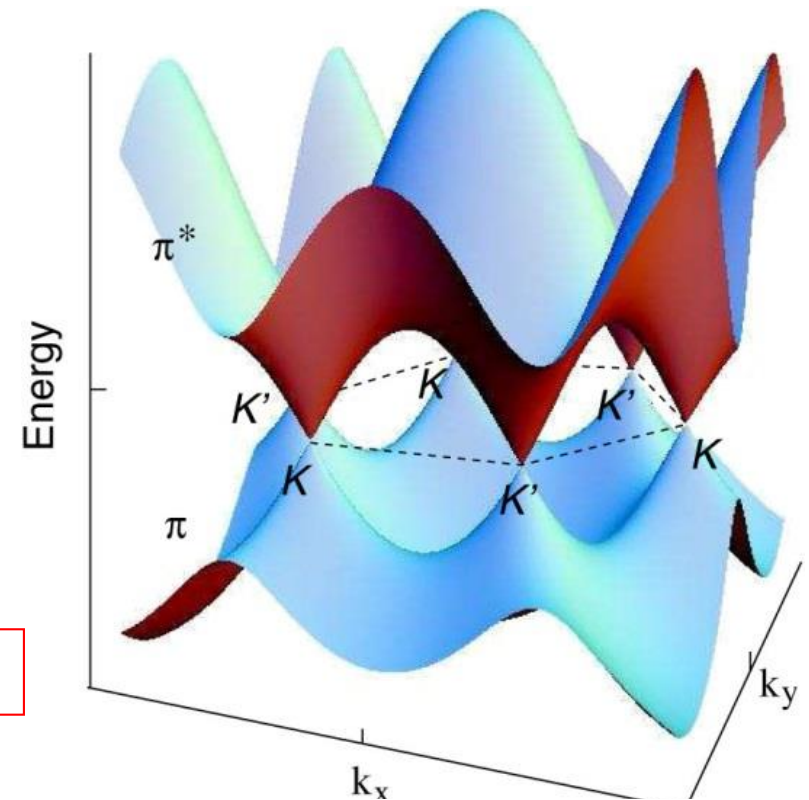
# Tight-binding model for electrons on the honeycomb lattice

$$H = \sum_{\mathbf{k}} \begin{pmatrix} a_{\mathbf{k}}^\dagger & b_{\mathbf{k}}^\dagger \end{pmatrix} h_{\mathbf{k}} \begin{pmatrix} a_{\mathbf{k}} \\ b_{\mathbf{k}} \end{pmatrix}$$

$$h_{\mathbf{k}} = \begin{pmatrix} 0 & f(\mathbf{k}) \\ f^*(\mathbf{k}) & 0 \end{pmatrix}$$

$$f(\mathbf{k}) = 1 + e^{-i\mathbf{k}\cdot\mathbf{a}_1} + e^{-i\mathbf{k}\cdot\mathbf{a}_2}$$

Dirac points at K and K'



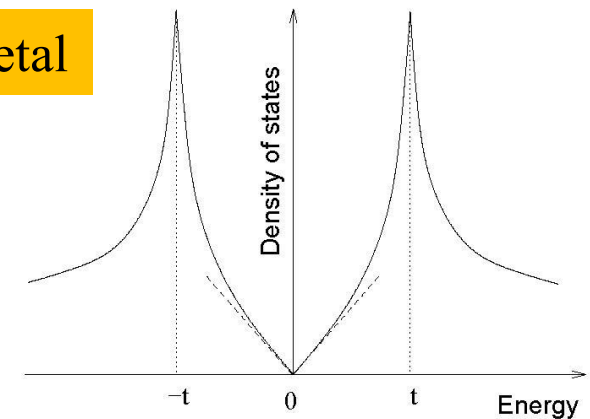
Energy bands:

$$\varepsilon_{\mathbf{k}}^\lambda = \lambda t \sqrt{1 + 4\cos\left(\frac{\sqrt{3}}{2}k_x a\right)\cos\left(\frac{3}{2}k_y a\right) + 4\cos^2\left(\frac{\sqrt{3}}{2}k_x a\right)}$$

$\lambda = \pm 1$ : band index

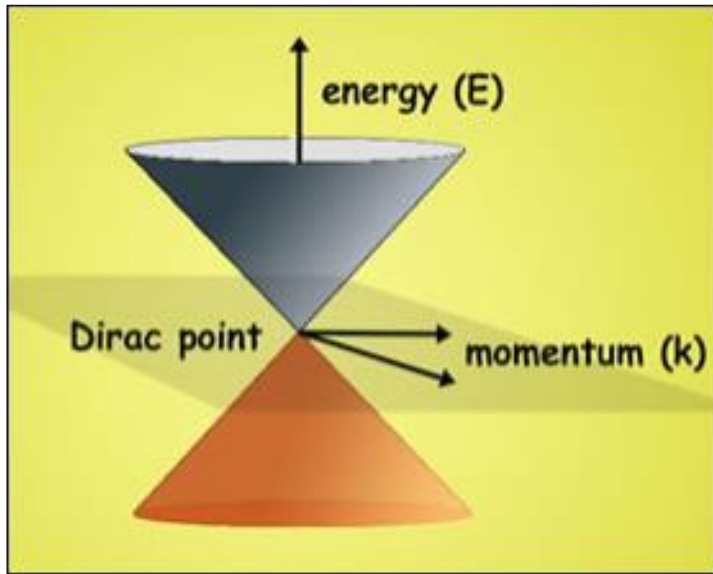
$$t \approx -3 \text{ eV}$$

Semi-metal





# Dirac points



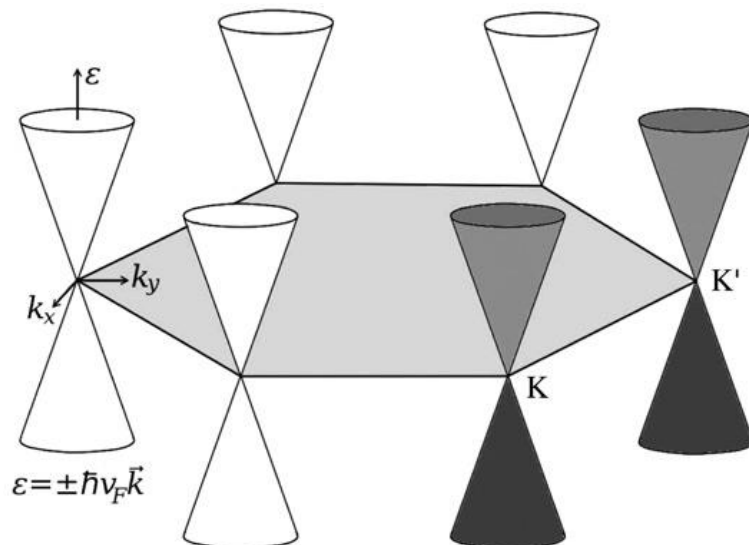
The Dirac points are situated at the points  $\mathbf{k}^D$  where

$$\varepsilon_{\mathbf{k}}^D = 0$$

Time-reversal symmetry:  $\varepsilon_{-\mathbf{k}} = \varepsilon_{\mathbf{k}}$

Dirac points occur in pairs:

**twofold valley degeneracy**



# Low-energy regime of the TB model: 2D Dirac equation

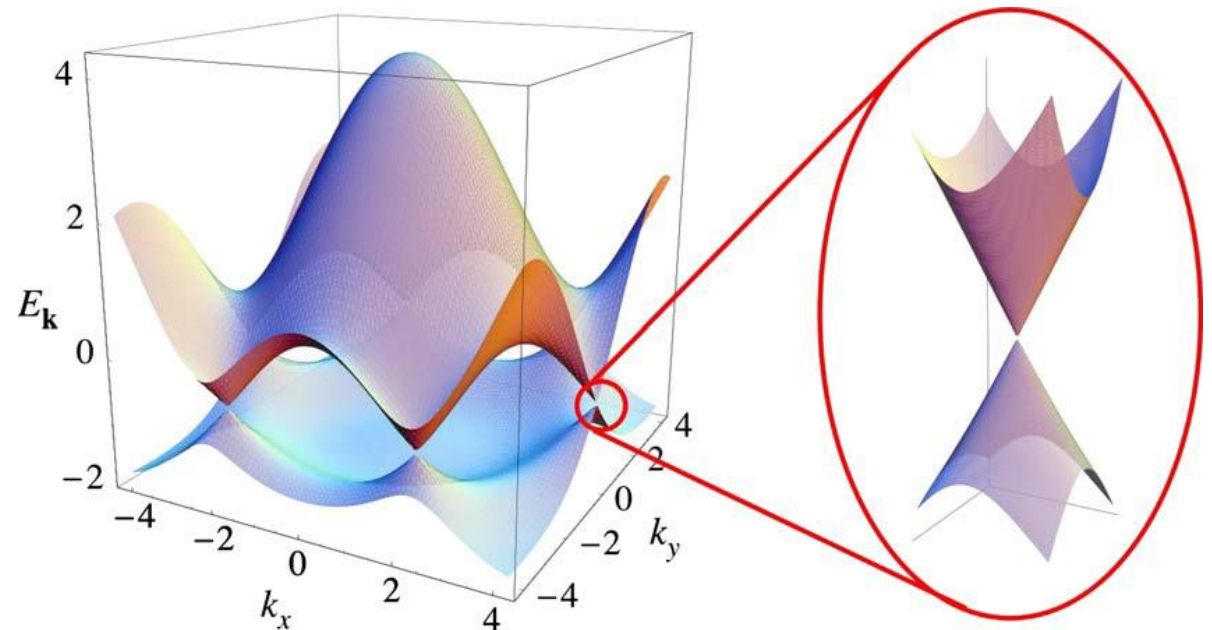
$$H_{\mathbf{q}}^{\xi} = \xi \hbar v_F \begin{pmatrix} 0 & q_x - iq_y \\ q_x + iq_y & 0 \end{pmatrix} = \xi \hbar v_F \mathbf{q} \cdot \boldsymbol{\sigma}$$

$\xi = \pm 1$  Valley pseudospin for K and K' points

$\boldsymbol{\sigma} = \sigma_x \hat{\mathbf{i}} + \sigma_y \hat{\mathbf{j}}$  Pauli matrices of the sublattice pseudospin

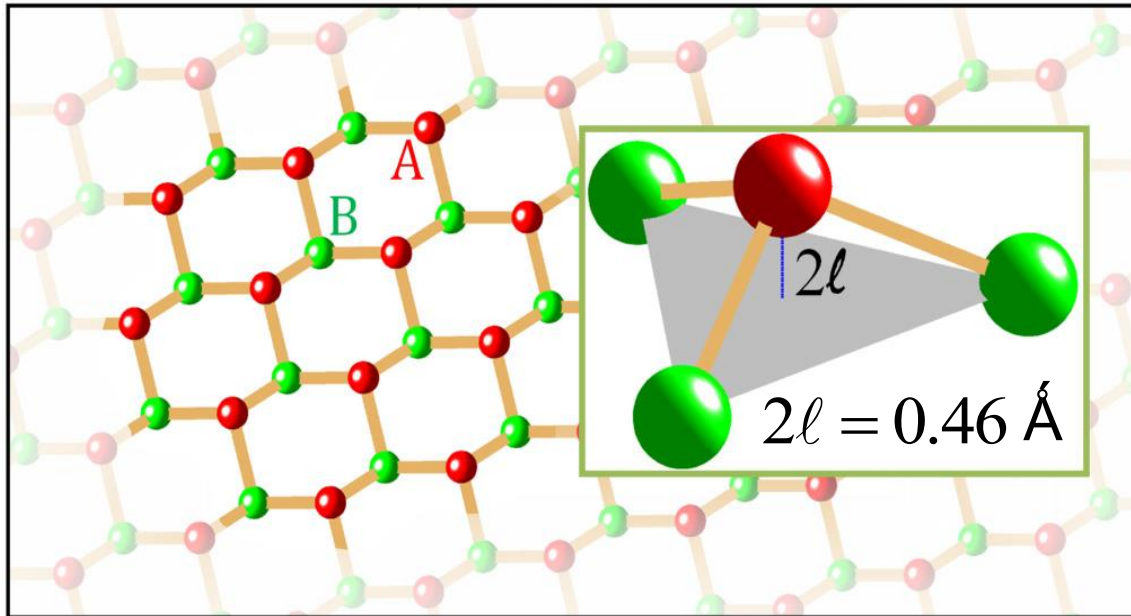
$$\varepsilon_{\mathbf{q},\xi}^{\lambda} = \lambda \hbar v_F |\mathbf{q}|$$

$$v_F = \frac{3|t|a}{2\hbar} \approx 8.7 \times 10^5 \text{ m/s}$$



# Transport in silicene

# Crystal structure of silicene



$$\lambda_{so} \approx 3.9 \text{ meV}$$

**Buckled structure**

- A potential difference  $\propto 2lE_z$  arises between silicon atoms at A sites and B sites when an electric field  $E_z$  is applied
- Energy gap 1.55 meV
- Silicene is compatible with silicon-based technology

# Low-energy Hamiltonian

$$H_{\xi} = \hbar v_F (\tau_x k_x - \xi \tau_y k_y) - \xi s_z \lambda_{so} \tau_z + \Delta_z \tau_z$$

$\xi = \pm 1$  valley index       $v_F \approx 5 \times 10^5 \text{ m/s}$  Fermi velocity

$\tau_i$  Pauli matrices of sublattice pseudospin

$\Delta_z = e\ell E_z$ ,       $E_z$  electric field

$s_z$  electron spin operator normal to silicene plane ( $s_z = \pm 1$ )

$\lambda_{so} \approx 3.9 \text{ meV}$  spin-orbit interaction

## Eigenfunctions

$$\Psi_{\lambda, \bar{k}, \xi, s_z}(\vec{r}) = \frac{1}{\sqrt{2S}} \begin{pmatrix} \sqrt{1 + \lambda \cos \theta} \\ \lambda \sqrt{1 - \lambda \cos \theta} e^{i\xi \phi_k} \end{pmatrix} e^{i\bar{k} \cdot \vec{r}}$$

## Eigenvalues

$$E_{\lambda, k, \xi, s_z} = \lambda \sqrt{\hbar^2 v_F^2 k^2 + (\Delta_z - \xi s_z \lambda_{so})^2}$$

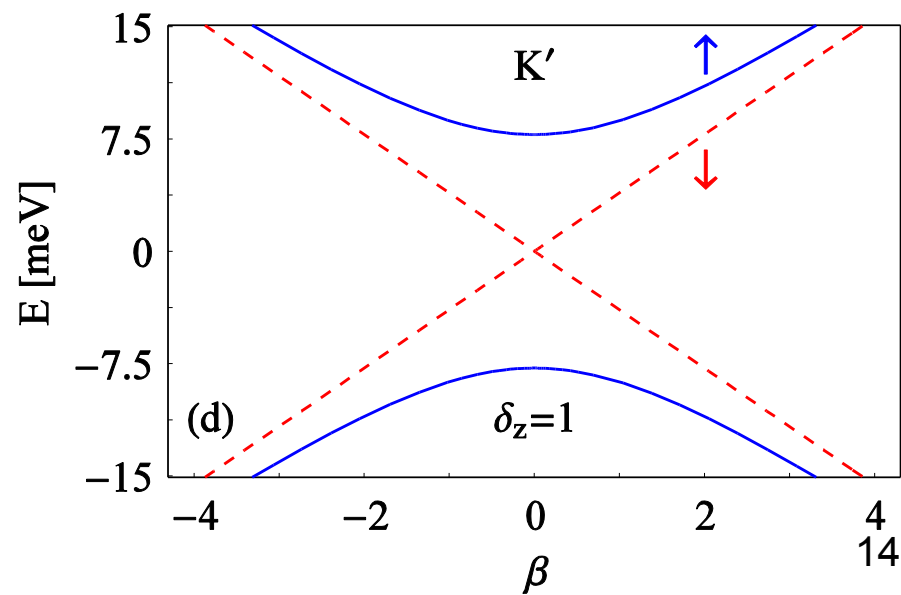
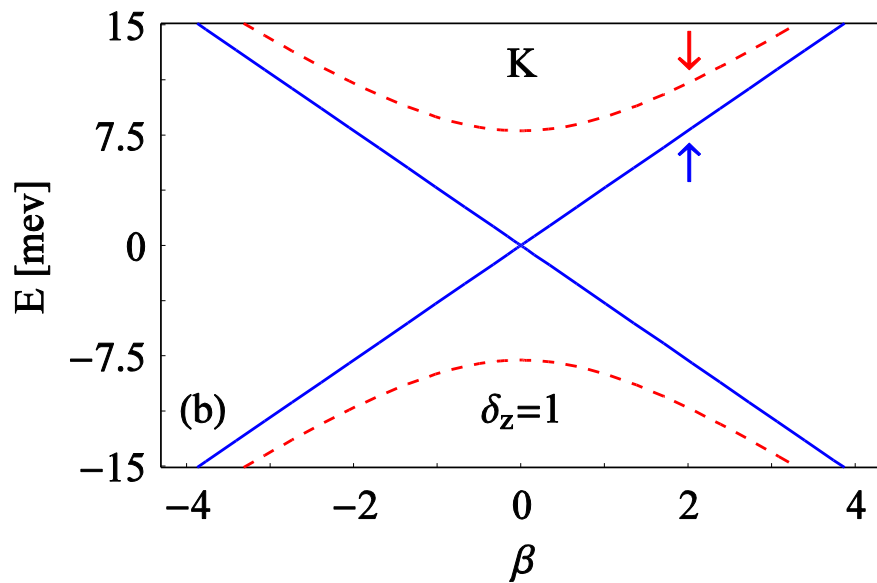
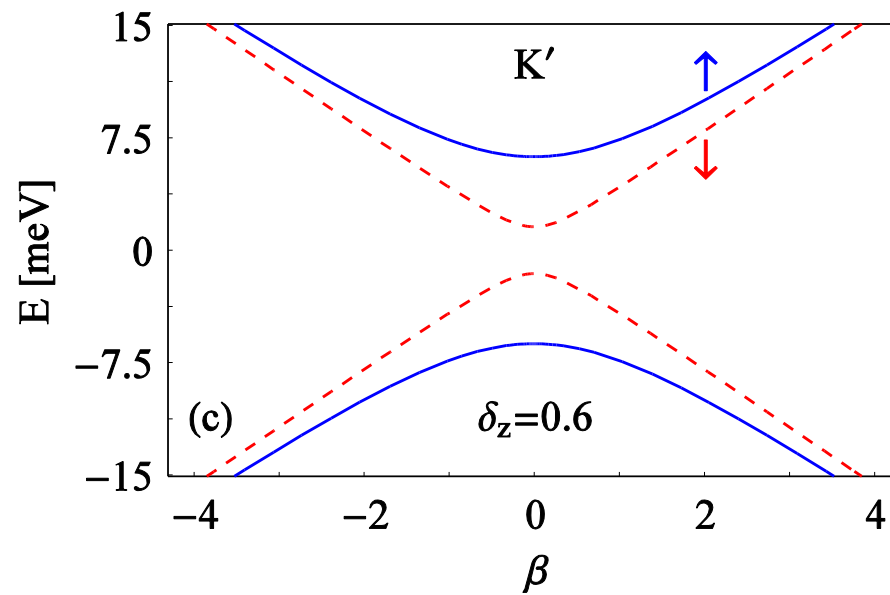
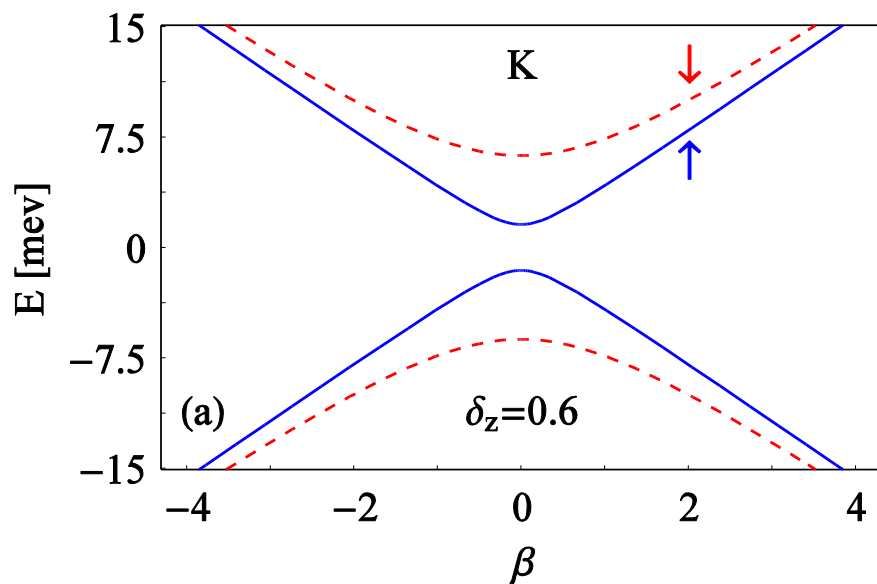
$\lambda = +1(-1)$  electron (hole) states

# Band structure

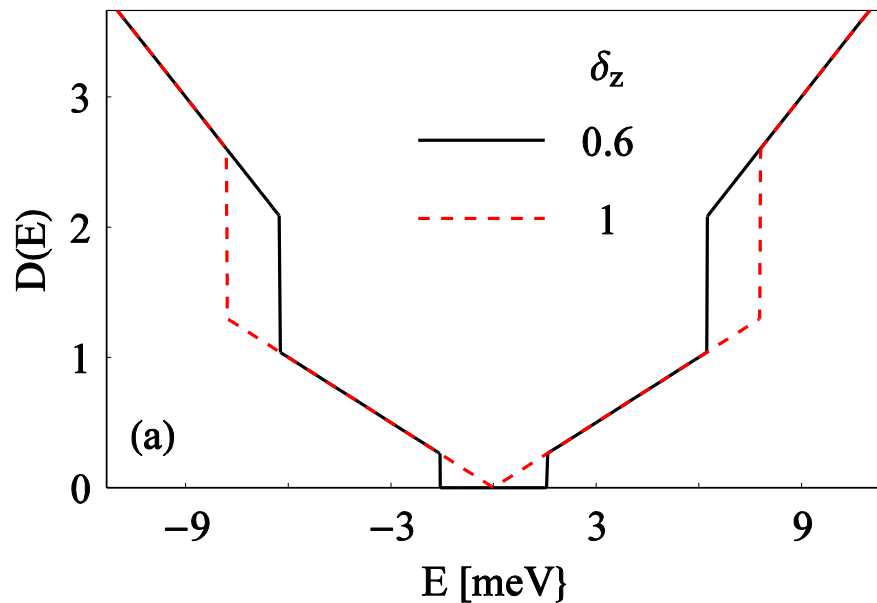
$$\delta_z = \Delta_z / \lambda_{so}$$

$$\beta = \hbar v_F k / \lambda_{so}$$

$$\delta_z = 1 \Leftrightarrow E_z = 0.17 \text{ V} / \text{nm}$$



# Density of states



$$D(E) = \frac{|E|}{\pi \hbar^2 v_F^2} \left[ \Theta(|E| - |\Delta_z - \lambda_{so}|) + \Theta(|E| - |\Delta_z + \lambda_{so}|) \right]$$

The DOS reflects the **two gaps** that open in the system

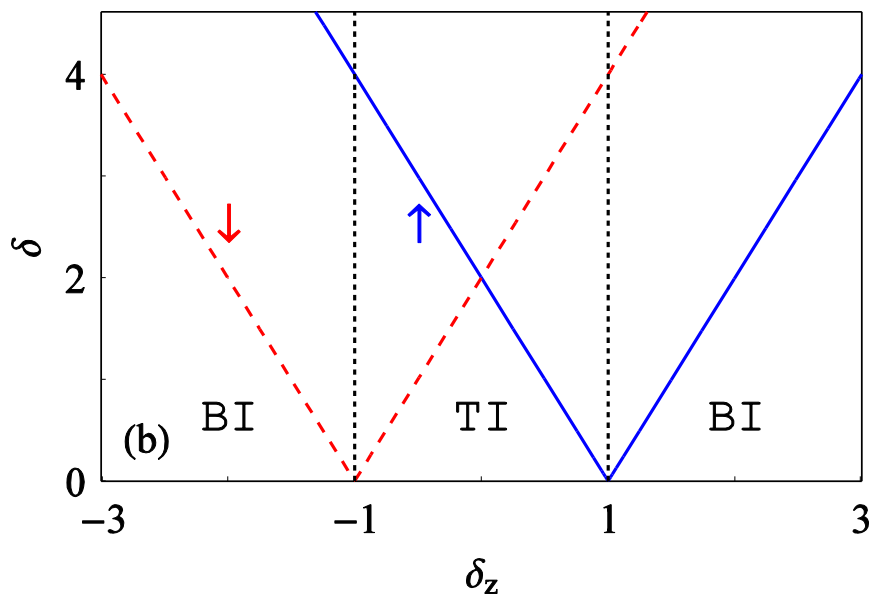
Evolution of the gap  $\delta$  with the electric field:

$$\delta = 2\lambda_{so} |\delta_z - \xi s_z|$$

The gap closes when  $\delta_z = \xi s_z = \pm 1$

This yields  $E_z = \xi s_z E_c$  with

$$E_c = \lambda_{so} / \ell = 17 \text{ meV/\AA}$$



# **Spin- and valley-polarized transport across ferromagnetic (FM) silicene junctions**



# Low-energy Hamiltonian

$$H_\xi = v_F (\tau_x p_x - \xi \tau_y p_y) + \Delta_{\xi s_z} \tau_z + U - s_z M \quad \text{with } \Delta_{\xi s_z} = \Delta_z - \xi s_z \lambda_{so}$$

Barrier potential  
(gate voltage)

Exchange field

Single **FM** junction  
**U, M**

## Eigenfunctions

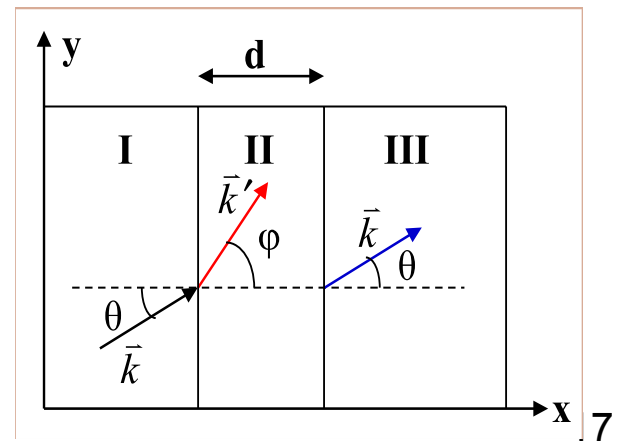
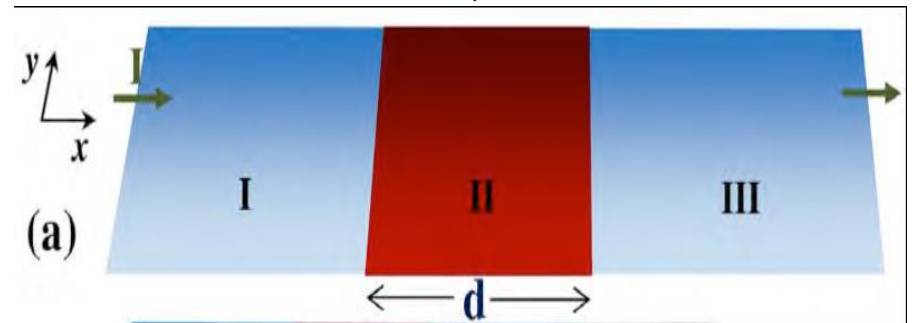
$$\Psi_I(\vec{r}) = A \begin{pmatrix} c_F e^{i\xi\theta} \\ E_N \end{pmatrix} e^{i\vec{k}\cdot\vec{r}} + rA \begin{pmatrix} -c_F e^{-i\xi\theta} \\ E_N \end{pmatrix} e^{i(-k_x x + k_y y)}$$

$$\Psi_{II}(\vec{r}) = a \begin{pmatrix} c'_F e^{i\xi\phi} \\ \varepsilon_F \end{pmatrix} e^{i\vec{k}'\cdot\vec{r}} + b \begin{pmatrix} -c'_F e^{-i\xi\phi} \\ \varepsilon_F \end{pmatrix} e^{i(-k'_x x + k'_y y)}$$

$$\Psi_{III}(\vec{r}) = tA \begin{pmatrix} c_F e^{i\xi\theta} \\ E_N \end{pmatrix} e^{i\vec{k}\cdot\vec{r}}, \quad A = 1/\sqrt{2E_F E_N}$$

Transmission amplitude

$$c_F = \hbar v_F k_F, \quad E_N = E_F + \xi s_z \lambda_{so}, \quad \varepsilon_F = E_F - U + s_z M - \Delta_{\xi s_z}$$



# Transmission and conductance through a FM junction

Incidence at an angle  $\theta$  :

$$T_{\xi s_z}(\theta) = \frac{\cos^2 \theta \cos^2 \phi}{\cos^2(k'_x d) \cos^2 \theta \cos^2 \phi + \sin^2(k'_x d) (\alpha + \alpha^{-1} - 2 \sin \theta \sin \phi)^2 / 4}$$

with  $\alpha = \varepsilon_F k_F / E_N k'_F$  and  $k'_x = \sqrt{k_F'^2 - k_F^2 \sin^2 \theta}$

Fermi wave vectors:

$$k_F = \frac{\sqrt{E_F^2 - \lambda_{so}^2}}{\hbar v_F} \quad k'_F = \frac{\sqrt{(E_F - U + s_z M)^2 - \Delta_{\xi s_z}^2}}{\hbar v_F}$$

$T_{\xi s_z}(\theta) = 1$  for  $k'_x d = n\pi$  as in graphene

Normal incidence  $\theta = 0$  :  $T_{\xi s_z}(0) = \frac{1}{1 + \sin^2(k'_x d) (\alpha - \alpha^{-1})^2 / 4}$

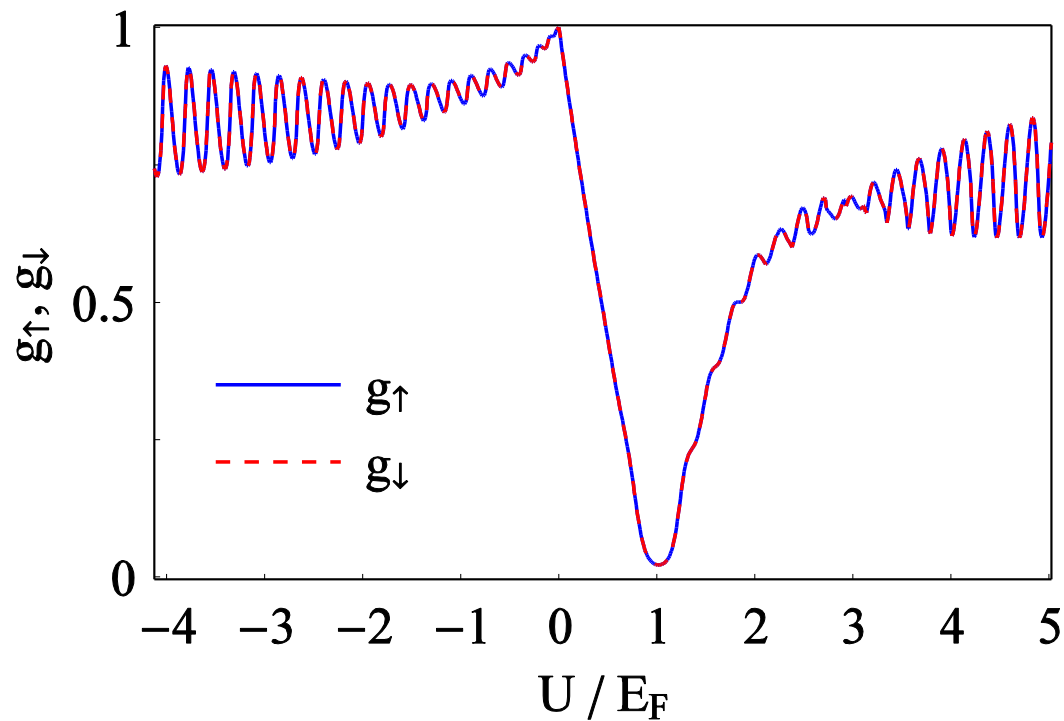
(in contrast to graphene  
it depends on barrier  
height)

Conductance:

$$G_{\xi s_z} = G_0 \int_{-\pi/2}^{\pi/2} T_{\xi s_z}(\theta) \cos \theta d\theta = G_0 g_{\xi s_z}, \quad G_0 = e^2 k_F W / 2\pi \hbar$$

$W$  sample width

# Spin-resolved conductance



$$\delta_z = 0, \quad m = M/E_F = 0$$

$$g_{\uparrow(\downarrow)} = \frac{g_{K\uparrow(\downarrow)} + g_{K'\uparrow(\downarrow)}}{2}$$

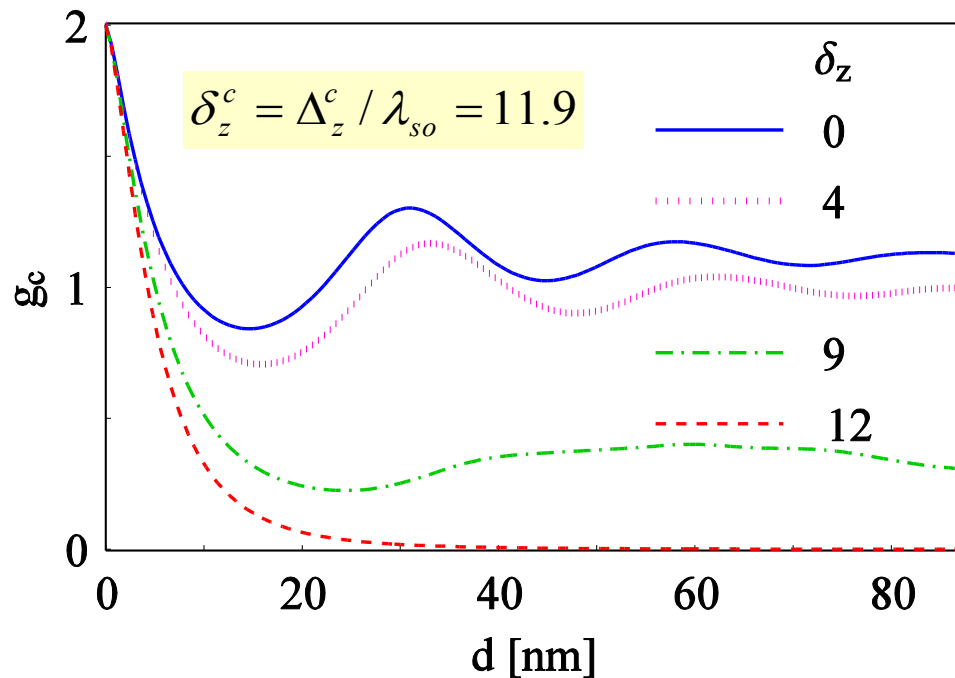
$$E_F = 40 \text{ meV}, \quad d = 110 \text{ nm}$$

Resonances for high barrier or deep well with amplitude between 2/3 and 1

Transport at the Dirac point (DP) is due to **evanescent modes**

Transport via evanescent modes is suppressed with increasing  $\delta_z$  and the dip develops to **transport gap**

# Tuning the conductance



$$g_c = g_{\uparrow} + g_{\downarrow}$$

$$U/E_F = 2, \quad M = 2.5 \text{ meV}$$

$$k'_x = \sqrt{k_F'^2 - k_F^2 \sin^2 \theta}$$

$k'_x$  becomes imaginary when  $k'_F$  becomes imaginary

$$\Delta_z^c = \xi s_z \lambda_{so} \pm |E_F - U + s_z M|$$

For  $\Delta_z > \Delta_z^c$  the Fermi level lies in the gap

No analog in graphene

In graphene  $\Delta_{\xi s_z} = 0$

$$\Rightarrow k'_F = |E_F - U| / \hbar v_F$$

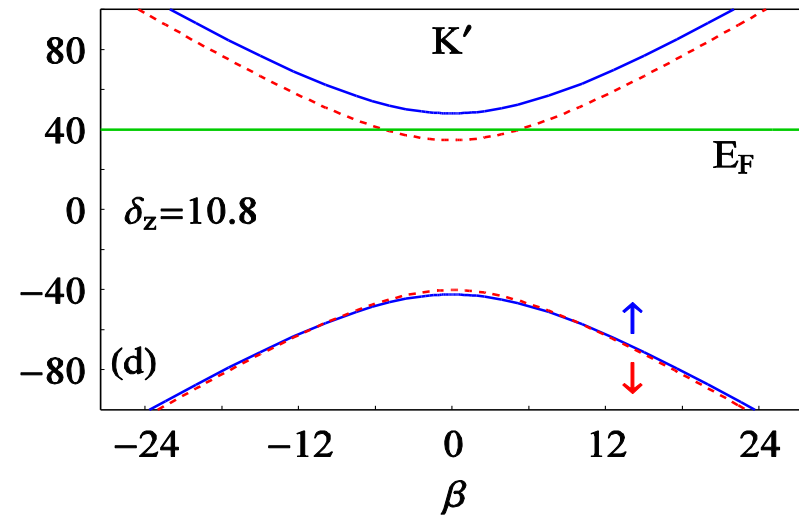
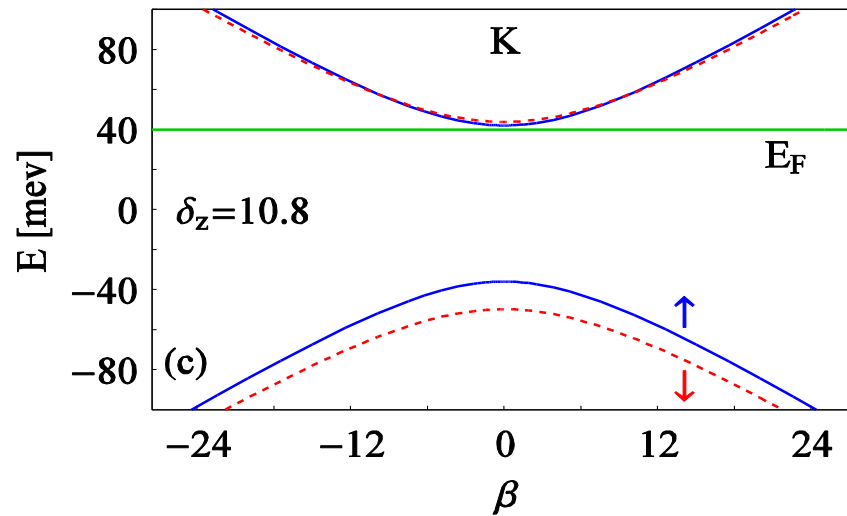
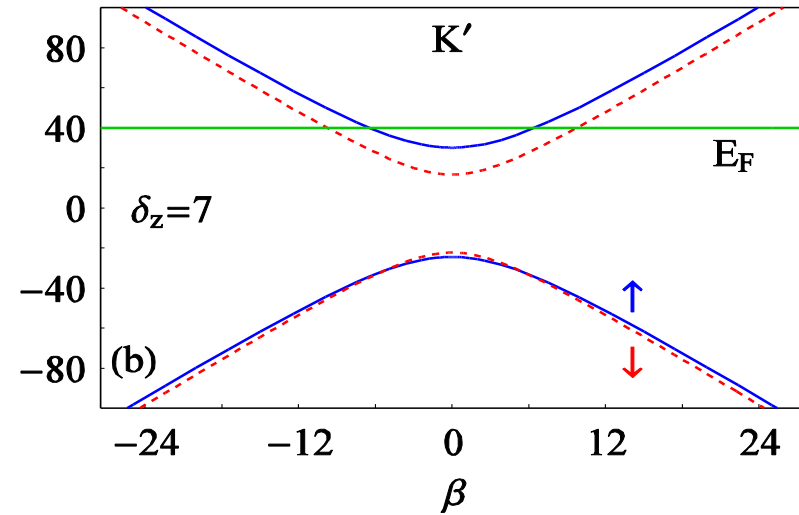
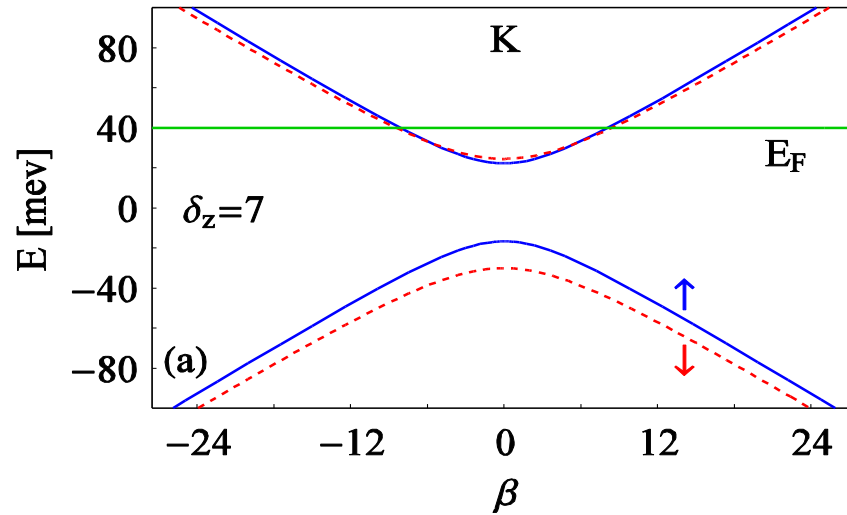
It cannot be made imaginary

The junction acts as an electric switch 20

# Band structure $M \neq 0$

$$\delta_z = \Delta_z / \lambda_{so}$$

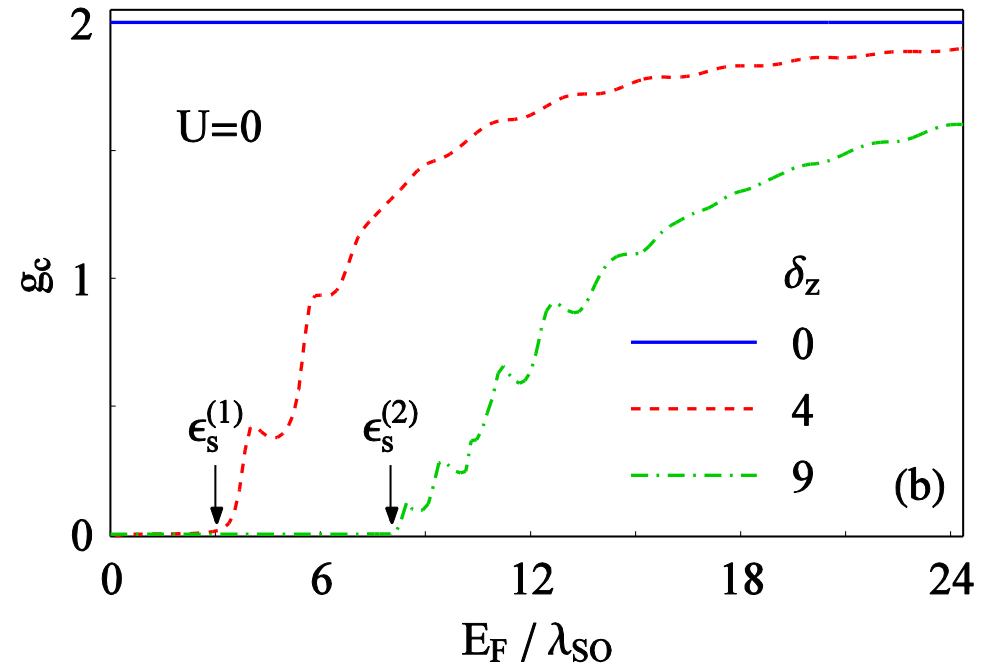
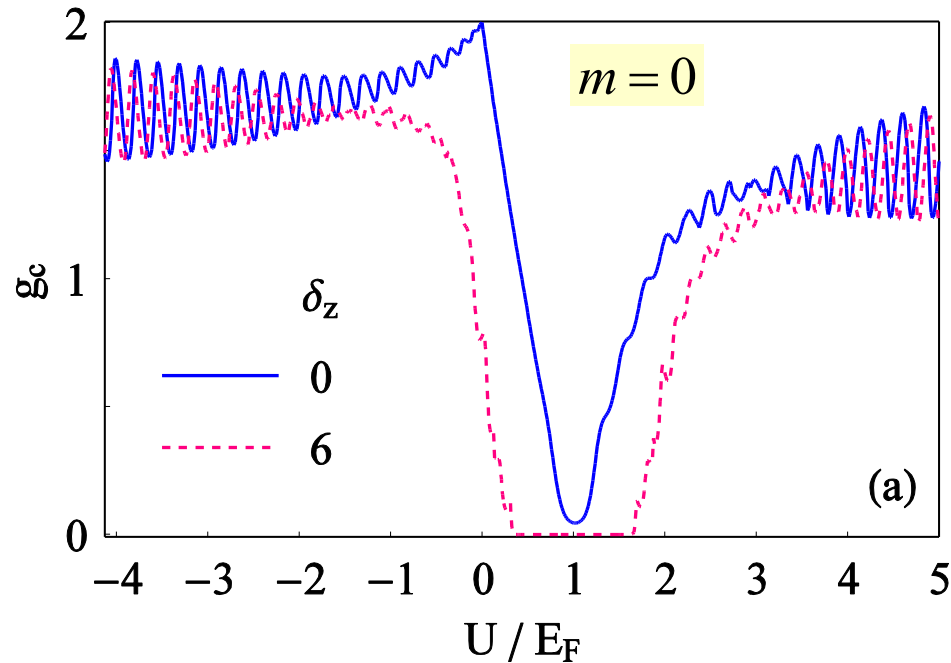
$$\beta = \hbar v_F k / \lambda_{so}$$



Current is entirely carried by **spin-down electrons** at the  $K'$  ( $g_{\downarrow}$  oscillatory)

Only **evanescent modes** contribute to  $g_{\uparrow}$  (monotonically decreasing behavior)<sup>21</sup>

# Conductance and transport gap



Near the DP  $k'_F$  is imaginary

$$\epsilon_s^{(1,2)} = E_F^{c(1,2)} / \lambda_{so}$$

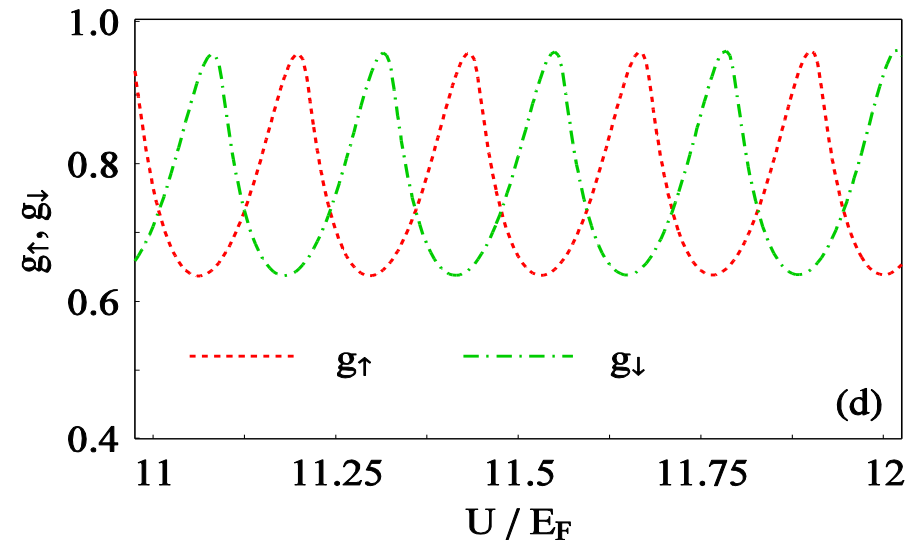
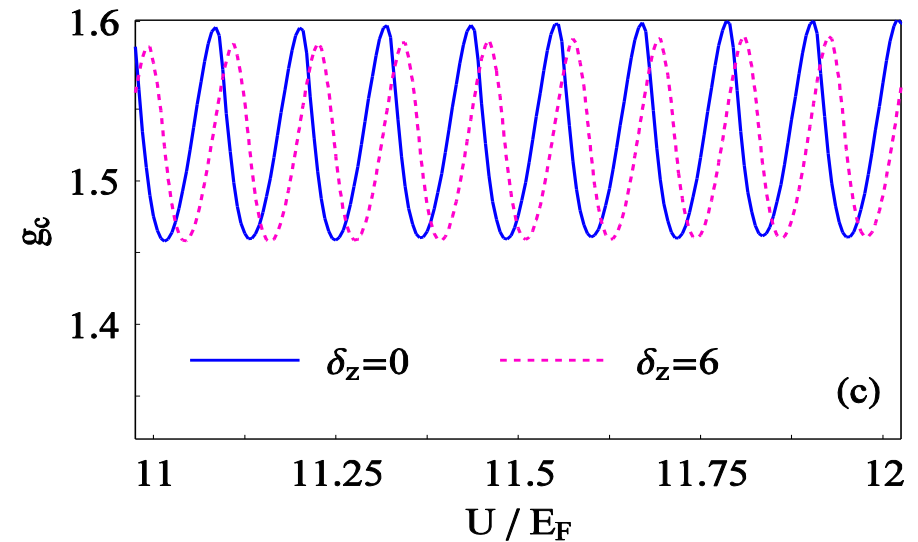
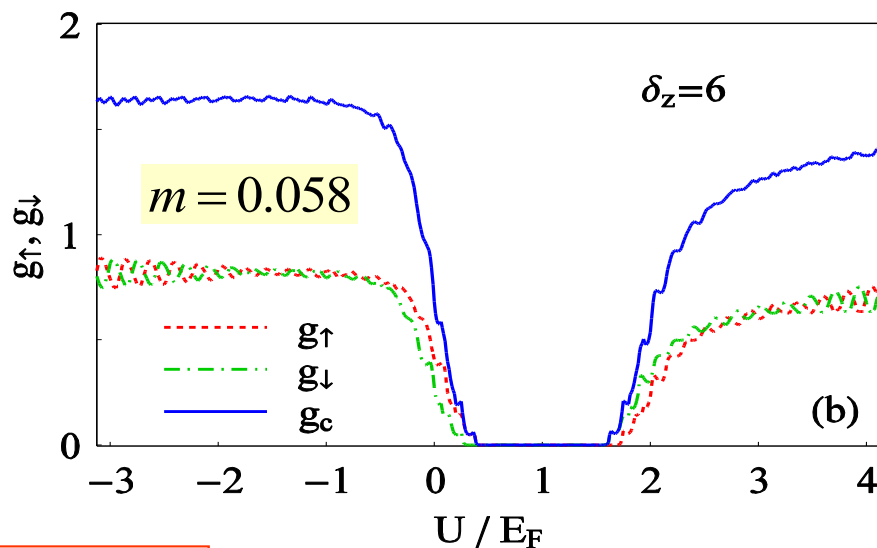
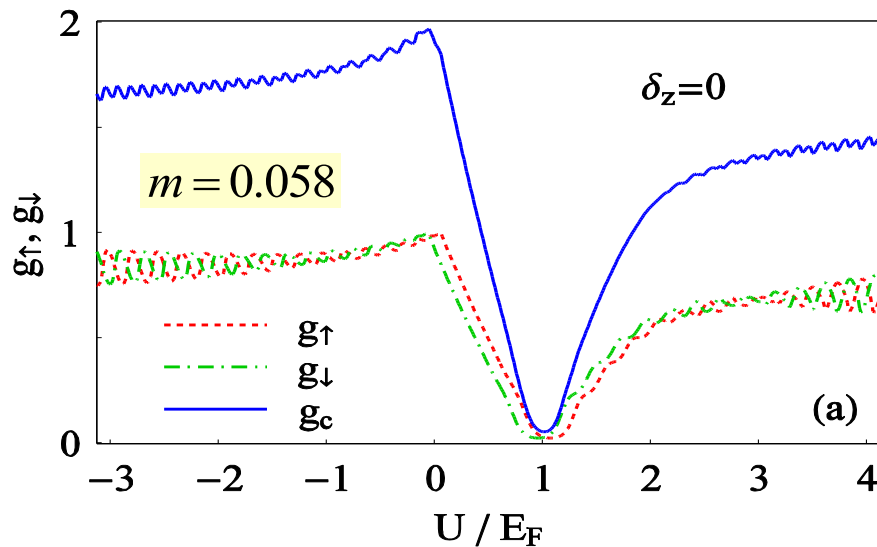
As  $\delta_z$  increases the evanescent modes are gradually damped out  $\Rightarrow$  **transport gap**

Transport gap when  $E_F < E_F^c$

$$E_F^c = \Delta_z - \lambda_{so}$$

**We aim now to explore possible spin and valley polarizations in FM silicene**

# Spin-resolved and charge conductances



$$m = M / E_F$$

Relative shift of  $g_{\uparrow}$  and  $g_{\downarrow}$  in the presence of  $M$   
 Transport gaps for both

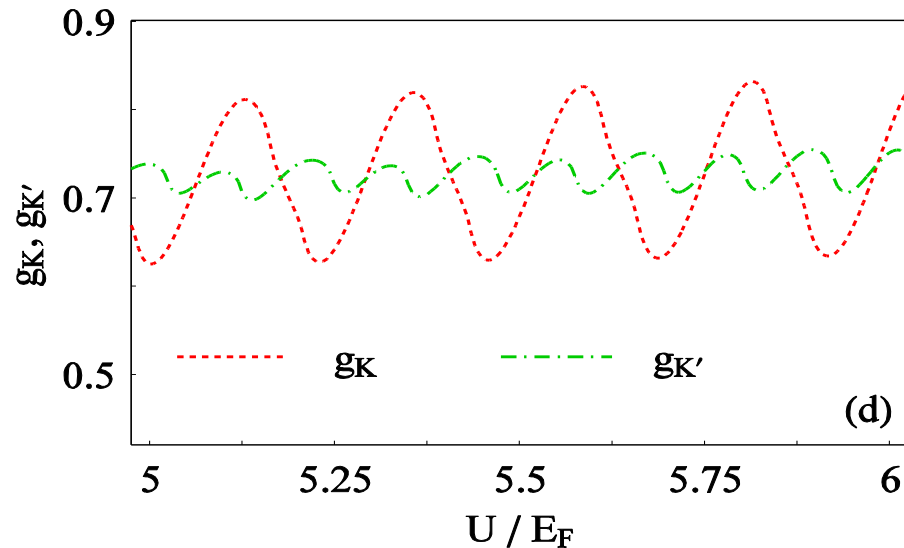
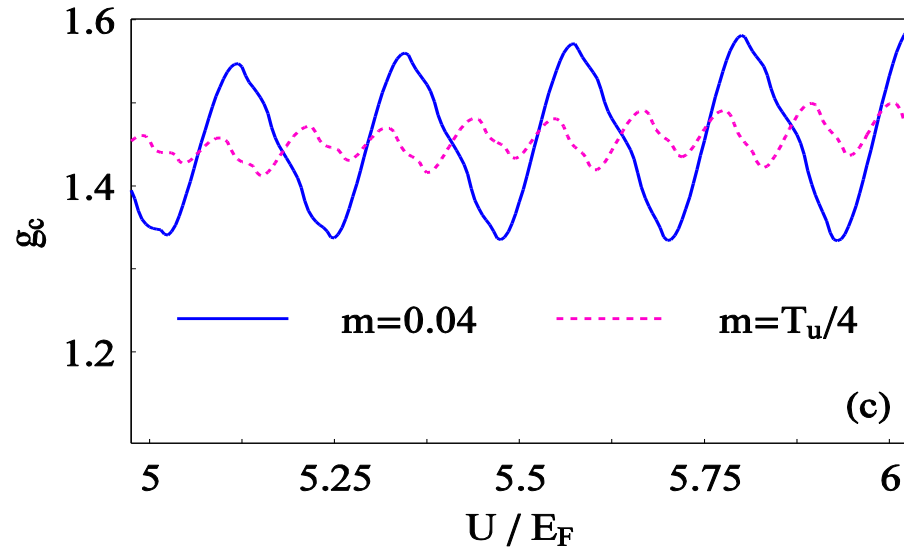
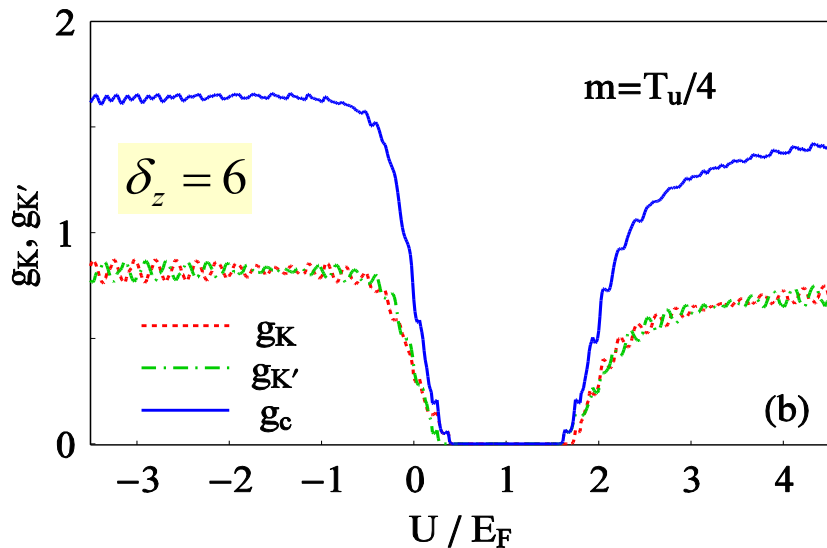
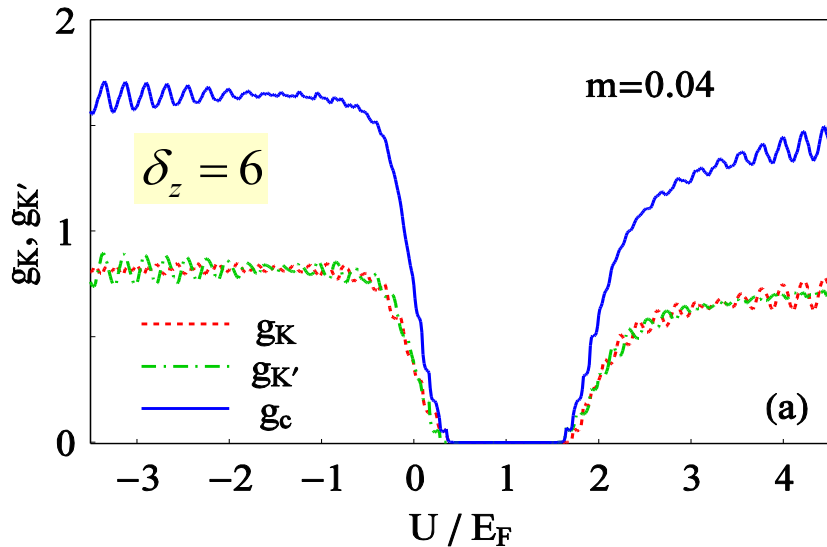
$g_c$  is periodic function of  $U/E_F$

$$T_u = \pi \hbar v_F / E_F d\delta_{\lambda} = 0.235$$

for  $|U/E_F| \gg 1$



# Valley-resolved and charge conductances

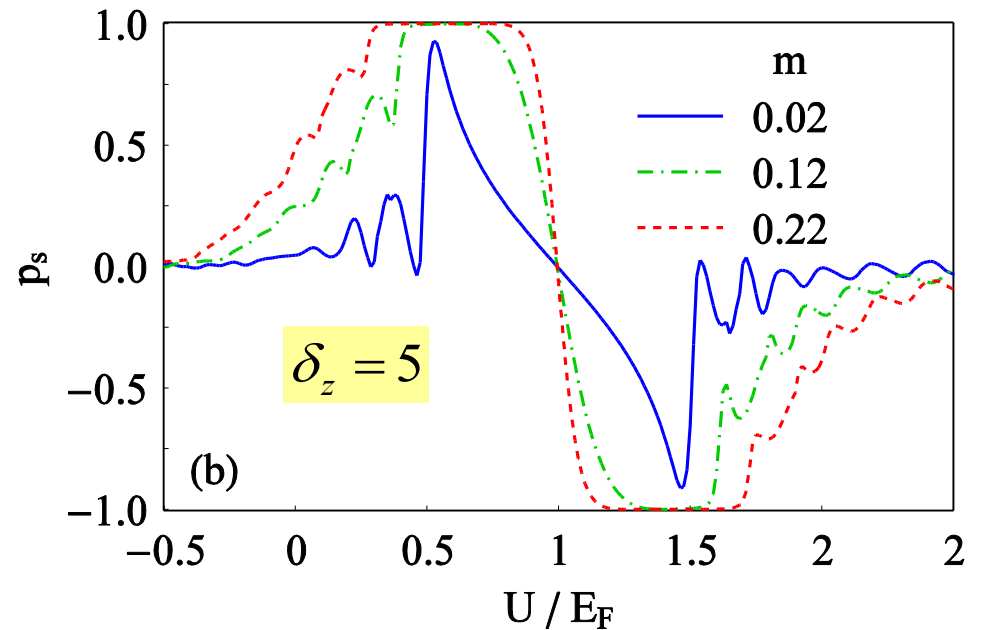
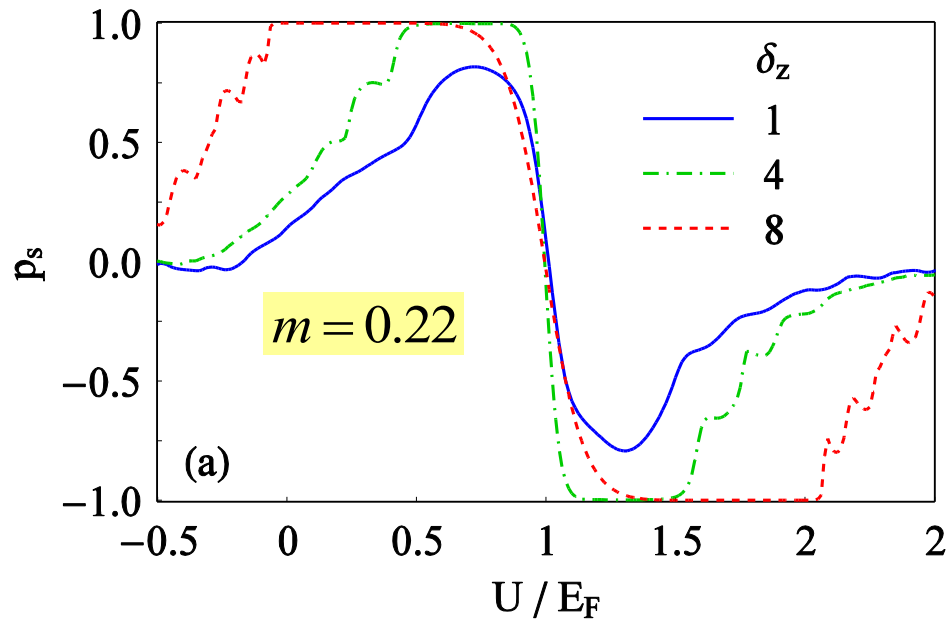


$$g_{K(K')} = \frac{g_{K(K')\uparrow} + g_{K(K')\downarrow}}{2}$$

Splitting of the peaks of  $g_c$  with  $m$

Splitting of the peaks of  $g_{K'}$  due to the **broken valley symmetry** in the presence of  $m$

# Spin polarization



$$p_s = \frac{g_\uparrow - g_\downarrow}{g_\uparrow + g_\downarrow}$$

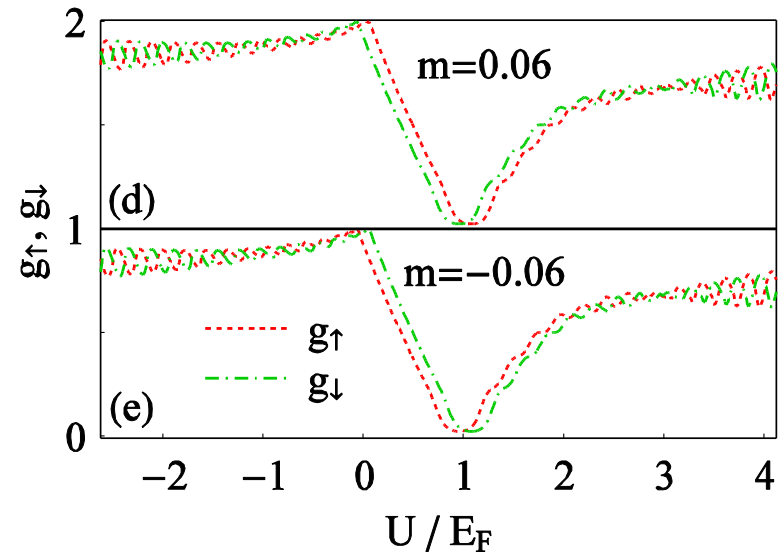
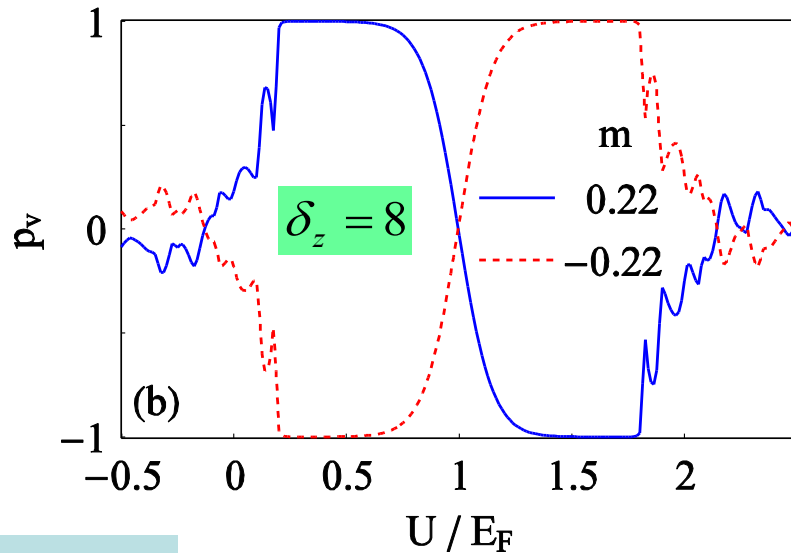
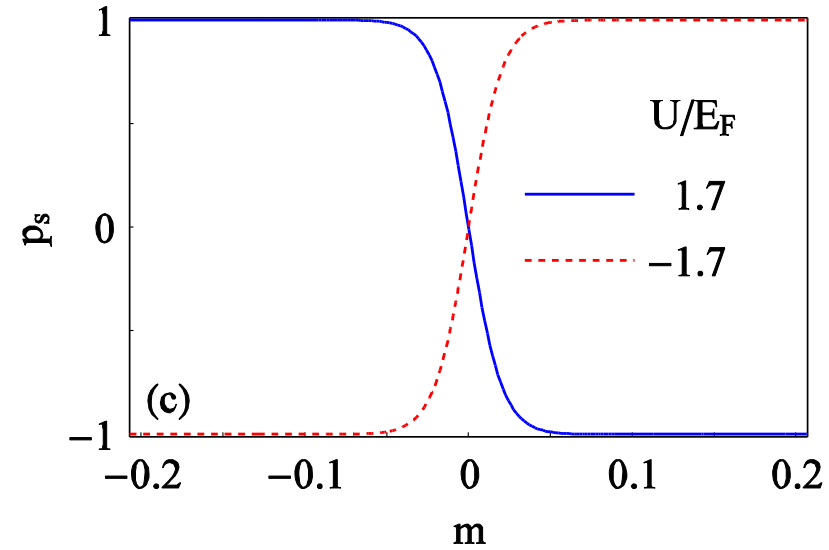
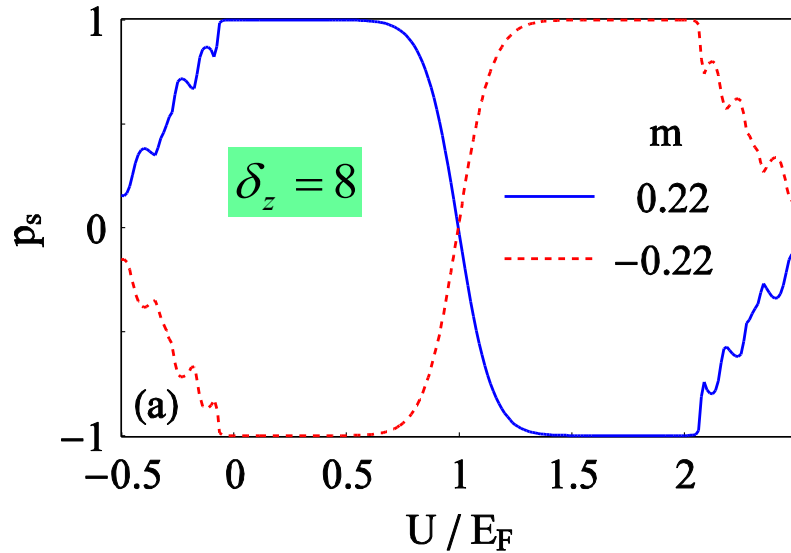
**The range of  $p_s \approx 1$  increases with  $\delta_z$  or  $m$**

For large  $\delta_z$  or  $m$ :

- only a **single spin band** contributes to the current
- the **evanescent modes** are suppressed
- the change of sign is due to the relative shift of  $g_\uparrow$  and  $g_\downarrow$

Spin polarization can be inverted by changing  $U$

# Spin and valley polarization



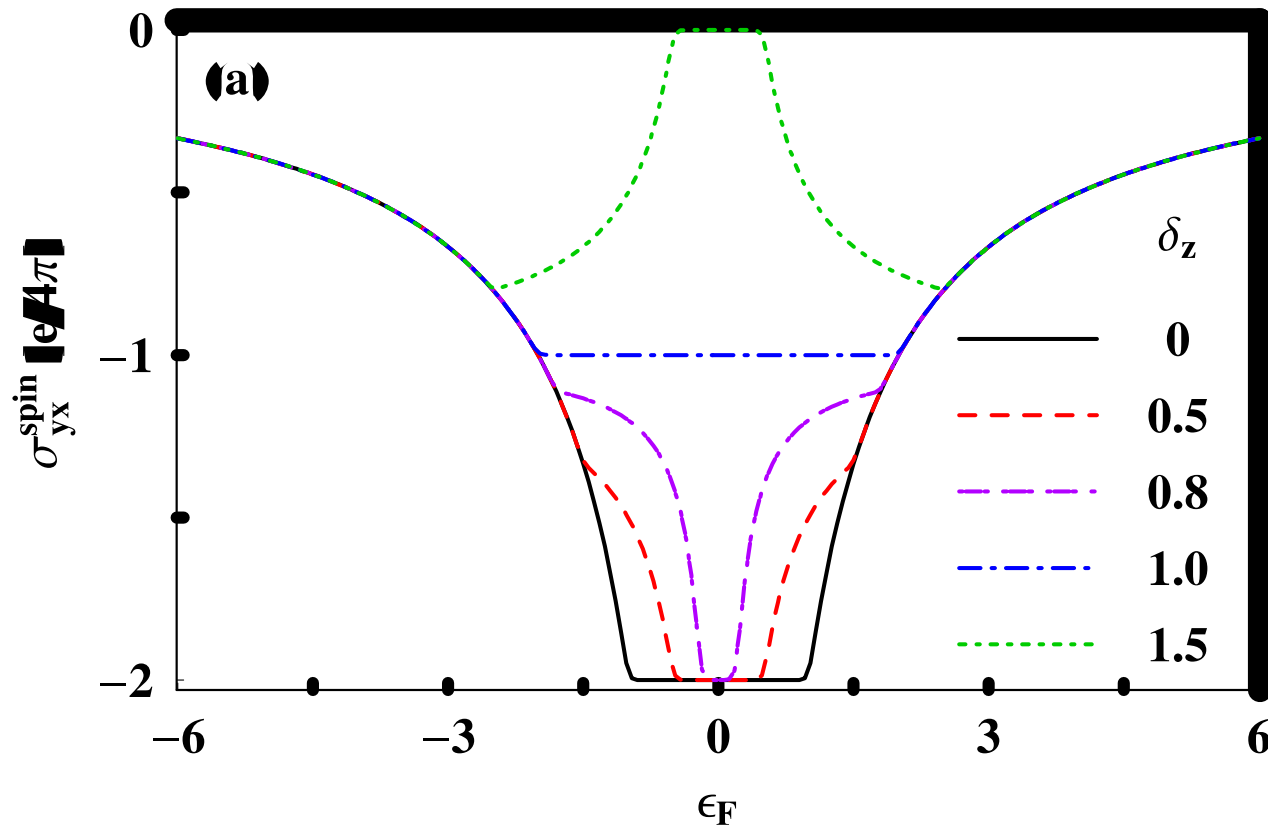
$$p_s = \frac{g_{\uparrow} - g_{\downarrow}}{g_{\uparrow} + g_{\downarrow}}$$

$p_s$  and  $p_v$  can be **inverted** by changing the direction of M

$$p_v = \frac{g_K - g_{K'}}{g_K + g_{K'}}$$

This is directly related to the relative shift of  $g_{\uparrow}$  and  $g_{\downarrow}$

# Transition from a topological insulator to band insulator regime



Spin-Hall conductivity becomes zero for high  $E_z$

The results for the polarized transport through a FM silicene junction can be used to realize silicene-based, high-efficiency spin- and valley-filter.

Other possible applications:

- In spintronics (due to longer spin-diffusion time and spin-coherence length)
- In quantum computing
- Silicene can overcome difficulties associated with potential applications of graphene in nanoelectronics (lack of a controllable gap)
- Optoelectronics
- Energy harvesting

# Summary

- The buckled structure of silicene can facilitate *the control of its band gap* by the application of an electric field  $E_z$ .
- Above a critical  $E_z$  the charge conductance  $g_c$  through a silicene FM junction changes from an *oscillatory to a monotonically decreasing function* of the junction width  $d$ . A gap develops near the DP with increasing  $E_z$ .
- These features can be used for the realization of **electric-field controlled switching**.
- The spin  $p_s$  and valley  $p_v$  polarizations near the DP increase with  $E_z$  or  $M$ , and become **nearly perfect** ( $\approx 100\%$ ) above certain  $E_z$  and  $M$  values.
- $p_s$  and  $p_v$  can be **inverted** by reversing the direction of  $M$  or  $U$ : **near perfect spin and valley filtering**

*Most of the results\* have no analog in graphene*

\*APL **105**, 223105 (2014), JAP **117**, 094305 (2015)